Chapter 5

PEGYLATION AND SURFACE FUNCTIONALIZATION

5.1 Materials

Anastrozole and exemestane were obtained as gift sample from Sun Pharma Advanced Research Company Ltd (SPARC), Vadodara, India. PLGA (lactide/glycolide ratio 50:50, Mol wt. 12 KDa) was obtained as a gift sample from Purac Biomaterials, Gorinchem, Netherlands. Poloxamer 188 was obtained as gift sample from BASF, Ludwigshafen, Germany. Capric/caprylic triglyceride (Capmul MCM, C8) was obtained as gift sample from Abitec Corporation, Janesville, USA. Caprolactone monomer was purchased from Sigma-Aldrich, Mumbai, India. Sulpho-NHS, 6-Coumarin was purchased from Sigma-Aldrich, Mumbai, India. Amine-PEG-carboxylic acid (Mol wt. 5000 Da) was purchased from Biomatrik, Jhegiang, China. Monoclonal antibody against estrogen receptor was purchased from Pierce antibodies, USA. THP1 cells were procured from NCCS, Pune, India. RPMI-1640, Fetal Bovine Serum (FBS), antibiotic-antimycotic, Trypsin-EDTA and PBS were purchased from Life Technologies Pvt. Ltd., New Delhi, India. 6-well plates, 96-well plates, tissue culture flask (25 and 75 cm^2), chamber slide and other sterile material for cell culture were purchased from Thermo scientific, India. EDC and NHS were purchased from Himedia, Vadodara, India. All other chemicals were of analytical reagent grade and obtained commercially.

5.2 Cell lines

Human acute monocytic leukemia cell line (THP1), was grown in RPMI-1640 medium (Gibco, Grand Island, NY, USA) supplemented with 5% (v/v) fetal bovine serum (FBS), penicillin (100 units/ml) and streptomycin (100 µg/ml) (Gibco, Grand Island, NY, USA) at 37 °C in a humidified incubator containing 5% CO_2.

5.3 Methods

5.3.1 Pegylation of nanoparticles

Pegylated nanoparticles (NPs) were prepared in similar manner as described in chapter 4 with replacement of a part of PLGA and PCL with PLGA-PEG and PCL-PEG, respectively. Five different formulations containing 0, 5, 10, 15 and 20% PLGA-PEG and PCL-PEG were prepared. Pegylated NPs were optimized based on percentage drug entrapment (PDE), particle size (PS) and phagocytic uptake studies on THP1 cells by flow cytometry. 6-Coumarin loaded NPs were also prepared in a similar way as reported previously in chapter 4 with addition of 6-Coumarin instead of ATZ/EXE. In

vitro drug release studies were performed as described in chapter 4 to compare any change in drug release due to pegylation.

5.3.2 Phagocytic uptake

Phagocytic uptake studies were performed using human acute monocytic leukemia cell line (THP1). 1 ml of THP1 cell suspension (2×10^5 cells) was incubated with 1 ml (200 µg/ml) of 6-Coumarin-loaded PLGA NPs, 6-Coumarin-loaded PCL NPs, pegylated PLGA NPs and pegylated PCL NPs (5, 10, 15, 20%) for 60, 120 and 240 min for phagocytic uptake. Cells were then centrifuged at 400×g for 5 min, re-suspended in 1× PBS and samples were analyzed using FACS. In FACS analysis, 10,000 cells were counted by measuring signal from FITC channel (FACS Canto-II, BD Biosciences, CA, USA) and analyzed by software provided with the instrument (BD FACS Diva 6.2.1 software, BD Biosciences, CA, USA).

5.3.3 Surface functionalization of NPs with ER antibody

For target specific drug delivery, coupling of ER antibody to NPs was carried out using a surface activation method [Acharya et al. 2009]. In brief, 10 mg of drug loaded NPs were dispersed in 2 ml of PBS (0.02 M, pH 7.4) followed by addition of 225 µl of EDC (1 mg/ml) and 140 µl of NHS (1 mg/ml) in to the above suspension. EDC activation was carried out by agitating the above suspension for 4 h at room temperature using a magnetic stirrer. Excess of un-reacted EDC and NHS were removed by size exclusion chromatography using Sephadex column and ER antibody (25 µl, 1 mg/ml) was added to the activated NPs. The above dispersion was agitated for 4 h at room temperature for conjugation of antibody to NPs. The prepared immunoNPs were characterized by PDE, PS, zeta potential and transmission electron microscopy.

5.4 Results and discussion

5.4.1 Physicochemical characterization of ATZ loaded PLGA NPs

ATZ loaded PLGA NPs were optimized for highest PDE and smallest PS as discussed in chapter 4. Optimized batch of ATZ loaded PLGA NPs had PDE of 62.09 ± 0.95%, PS of 145.9 ± 2.3 nm and zeta potential of -30.7 ± 1.4 mV.

5.4.2 Optimization of ATZ loaded PLGA NPs containing different PEG ratio based on PDE, PS and phagocytic uptake studies

ATZ loaded pegylated NPs were optimized based on PDE, PS and phagocytic uptake studies on THP1 cells by FACS. Physicochemical parameters of formulations with

different PEG content are summarized in table 5.1. From the results, it was observed that as the amount of PEG increased, PDE, PS and zeta potential decreased. However, the decrease in PDE, PS or zeta potential were not significant ($p>0.01$). Decrease in PS was possibly due to the presence of both hydrophilic (PEG) and hydrophobic (PLGA) end in PLGA-PEG, imparting amphiphilic nature to NPs [Avgoustakis et al. 2003; Chaudhari et al. 2012a; Chaudhari et al. 2012b; Ramanlal Chaudhari et al. 2012]. Decrease in PDE was possibly due to decreased size of the NPs and decrease in zeta potential was due to increase in PEG chains on the surface of NPs.

Table 5.1 Physicochemical characterization of ATZ loaded PLGA NPs, pegylated PLGA NPs and ImmunoNPs

Formulation	PDE (%)	PS (nm)	Zeta Potential (mV)
PLGA NPs	62.09 ± 0.95	145.9 ± 2.3	-30.7 ± 1.4
PLGA-PEG NPs (5%)	62.21 ± 1.07	142.3 ± 3.5	-31.8 ± 2.3
PLGA-PEG NPs (10%)	61.98 ± 0.87	137.7 ± 3.1	-28.6 ± 1.9
PLGA-PEG NPs (15%)	61.76 ± 1.15	135.9 ± 2.7	-24.0 ± 2.7
PLGA-PEG NPs (20%)	61.36 ± 0.99	126.6 ± 4.1	-24.1 ± 3.4
ImmunoNPs	60.85 ± 1.53	140.4 ± 3.7	-23.6 ± 4.0

The process of phagocytosis commences by two ways, first is by protein adsorption and second is by secretion of pro-inflammatory cytokines. Kanchan et al demonstrated that in vitro phagocytosis process can be simulated using macrophage cell line. After incubation of NPs with macrophage cell line, secretion level of IFN-c and IL-4 increases [Kanchan and Panda 2007; Muhlfeld et al. 2007]. 6-Coumarin is a well known fluorescent probe and is used to study phagocytic uptake of prepared NPs due to its low pH dependent solubility and good fluorescence. Here, relative uptake of 6-Coumarin loaded NPs (pegylated and non-pegylated) in human acute monocytic leukemia cell line (THP1) was performed to confirm their in vitro anti-opsonization activity. Phagocytic uptake of PLGA NPs was compared with pegylated NPs containing varied quantity of PLGA-PEG (5, 10, 15 and 20%) in terms of mean fluorescence intensity after 60, 120 and 240 min as shown in figure 5.1 (a), (b) and (c), respectively. Pegylated NPs displayed greater resistance to phagocytic uptake than non-pegylated NPs. After 60 min, uptake of

PLGA NPs was 1.32, 2.38 and 9.34 times more than PLGA-PEG (5%), PLGA-PEG (15%) and PLGA-PEG (20%) NPs (figure 5.2). When phagocytic uptake of NPs was studied at three different time points, it was found that phagocytosis increased in a time dependent manner. However, overall uptake decreased with increase in PEG content due to increased hydrophilicity of NPs. These results are in accordance with earlier reports [Chaudhari et al. 2012c; Mosqueira et al. 1999]. The uptake of PLGA NPs is also affected by their surface charge. Cationic particles are more efficiently up taken by phagocytes as compared to negatively charged particles. This is because the ionic attraction between the positively charged particles and negatively charged cell surface causes efficient binding and facilitate the internalization process [Josephson et al. 1999]. As pegylated NPs exhibited negative zeta potential (-24.1 ± 3.4 mV), we can assume that they will successfully avoid phagocytosis and hence will be long circulating.

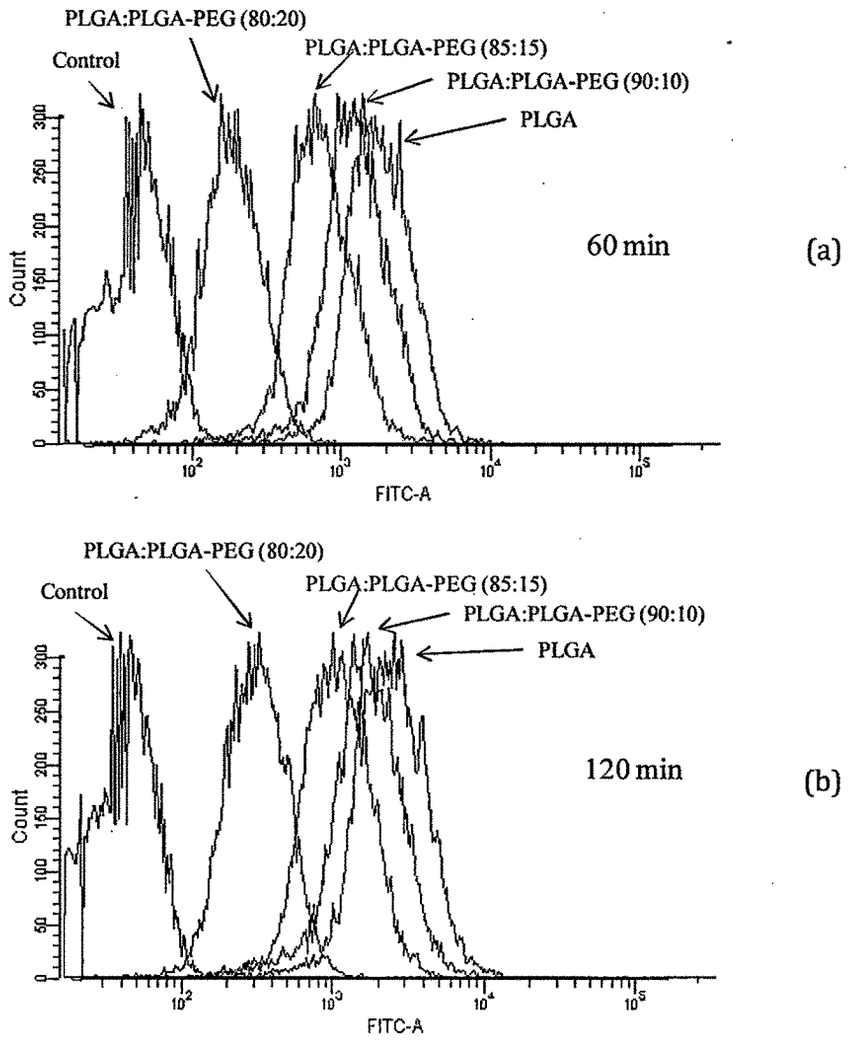

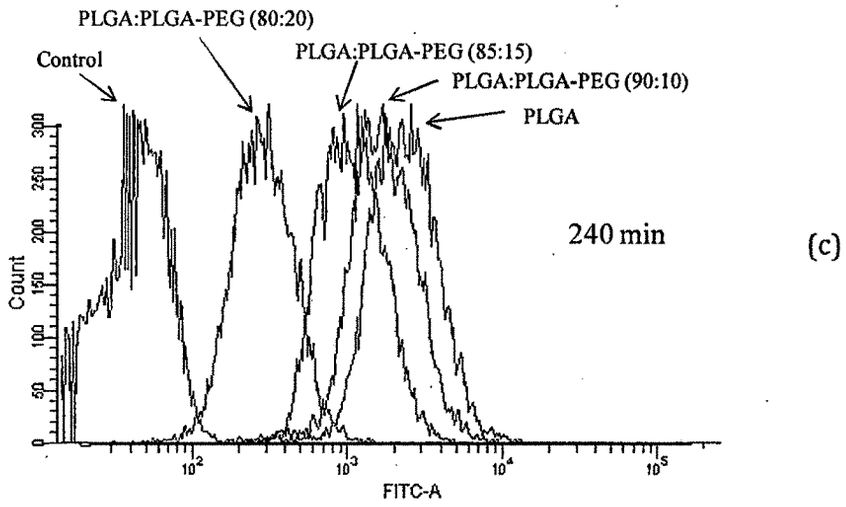

Figure 5.1 Phagocytic uptake histograms of 6-Coumarin loaded NP formulations by human acute monocytic leukemia cell line (THP1) after incubation for (a) 60, (b) 120 and (c) 240 min using FACS.

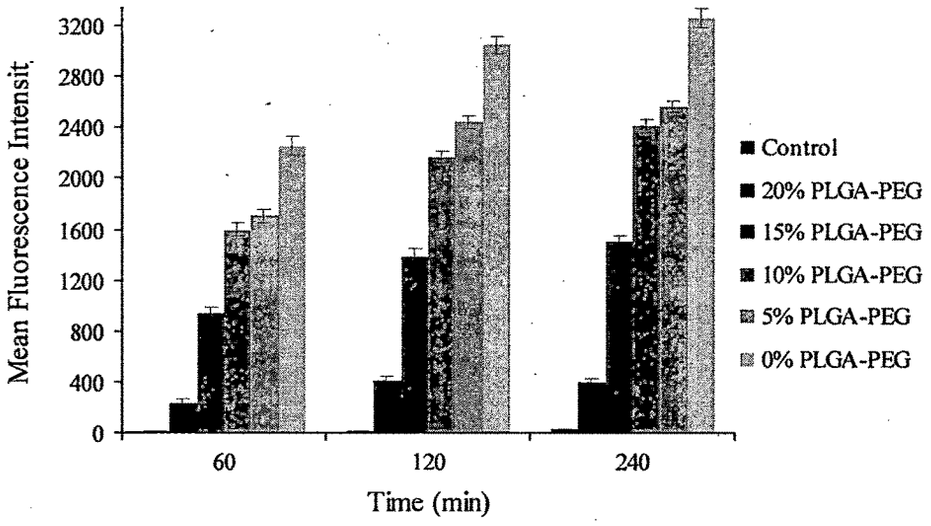

Figure 5.2 Phagocytic uptake of 6-Coumarin loaded PLGA and pegylated PLGA NPs using Human acute monocytic leukemia cell line, THP1 after incubation for 60, 120 and 240 min using FACS. Data presented as Mean ± SD, n=3

The in vitro drug release studies from different nanoparticulate formulations were performed in PBS pH 7.4. Pegylated NPs showed faster release as compared with non-pegylated NPs. In vitro release of ATZ from drug suspension and NPs is shown in figure 5.3. Within 3 h, 82.56 ± 0.623% drug release occurred from plain drug suspension, whereas only 24.14 ± 0.316% and 28.90 ± 1.03% drug released from PLGA and pegylated PLGA NPs, reaching 48.02 ± 0.566% and 60.29 ± 0.85% after 120 h and 64.9 ±

0.249% and 83.04 ± 0.55% after 240 h, respectively, indicative of sustained release. The drug release from NPs followed biphasic release model with an initial burst release for about 3 h followed by sustained release for more than 240 h. Pegylated PLGA NPs showed faster release of drug when compared to PLGA NPs due to the presence of hydrophilic PEG chains around the NPs, causing increased diffusion of water to the core of particles. The regression coefficient of the plot of log M_t/M_∞ versus log t was found to be 0.948 and 0.956 with value of release exponent (n) as 0.255 and 0.264, respectively for PLGA and pegylated PLGA NPs. The n value is the release exponent which characterizes the transport mechanism and if its value is less than 0.5, it indicates Fickian release. Hence, it can be concluded that the release of ATZ from NPs was by Fickian diffusion.

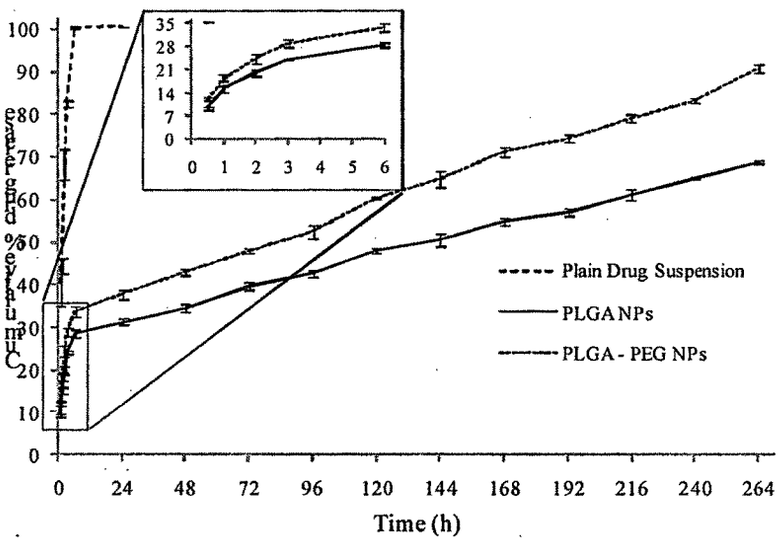

Figure 5.3 Drug release profile of ATZ from plain drug suspension, PLGA NPs and pegylated PLGA NPs across semi-permeable membrane using the dialysis bag diffusion technique in phosphate buffered saline (pH 7.4). The values represent mean ± S.D. of three batches.

5.4.3 Physicochemical characterization of ImmunoNPs

ATZ loaded pegylated PLGA NPs were conjugated with anti-estrogen receptor monoclonal antibody for targeting breast tumor by two-step EDC-NHS activation method. In this method, amino group of monoclonal antibody was conjugated to carboxyl groups of PEG through an amide bond formation [Kocbek P 2007]. It was estimated that approximately 54 Ab molecules were present on each NP [Olivier et al. 2002].

ATZ was successfully loaded in pegylated PLGA NPs prior to Ab conjugation (61.29 ± 1.18%) and no significant loss in drug content was observed after surface functionalization with Ab (60.62 ± 0.54%). However, slight increase in PS was observed which increased from 126.6 ± 4.1 to 140.4 ± 3.7 nm with no significant change in zeta potential from -24.1 ± 3.4 to -23.6 ± 4.0 mV. Poly dispersity index before and after Ab conjugation was less than 0.1 indicating mono-dispersity of particles. A similar trend was observed by Das et al. and Tseng et al. when they conjugated antibody on PLGA and gelatin NPs, respectively [Das and Sahoo 2011; Tseng et al. 2007]. TEM image showed discrete spherical particles with monodisperse size of about 100 nm (figure 5.4). The higher hydrodynamic diameter of NPs achieved by dynamic light scattering (Zetasizer NanoZS) analysis as compared to the size obtained by TEM analysis is possibly contributed by the hydration of the surface associated PEG.

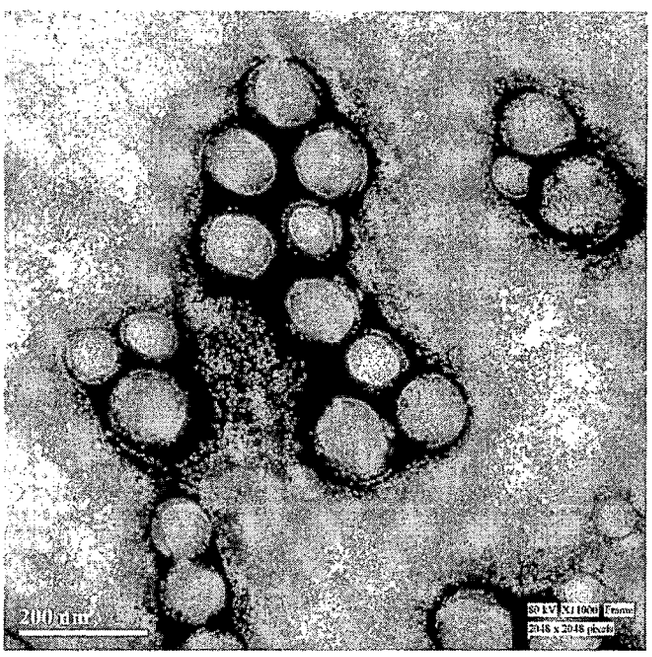

Figure 5.4 TEM image of ATZ loaded pegylated PLGA ImmunoNPs.

5.4.4 Physicochemical characterization of EXE loaded PCL NPs

EXE loaded PCL NPs were optimized for highest percentage drug entrapment (PDE) and smallest particle size (PS) as discussed in chapter 4. Optimized batch of EXE loaded PCL NPs had PDE of 84.07 ± 2.02%, PS of 182.6 ± 3.8 nm and zeta potential of -33.8 ± 2.1 mV.

5.4.5 Optimization of EXE loaded PCL NPs containing different PEG ratio based on PDE, PS and phagocytic uptake studies

Physicochemical parameters of NPs with different PEG content are summarized in table 5.2. From the results, it was observed that as the amount of PEG increased, PDE, PS and zeta potential decreased. However, the decrease in PDE, PS or zeta potential were not significant ($p<0.01$).

Table 5.2 Physicochemical characterization of EXE loaded cPCL NPs, pegylated PCL NPs and ImmunoNPs

Formulation	PDE (%)	PS (nm)	Zeta Potential (mV)
PCL NPs	84.07 ± 2.02	182.6 ± 3.8	-33.8 ± 2.1
PCL-PEG NPs (5%)	84.12 ± 1.12	184.1 ± 2.4	-33.3 ± 1.6
PCL-PEG NPs (10%)	83.58 ± 1.25	179.1 ± 4.1	-31.7 ± 1.3
PCL-PEG NPs (15%)	83.20 ± 0.92	173.7 ± 3.5	-29.6 ± 3.1
PCL-PEG NPs (20%)	82.73 ± 1.19	168.9 ± 2.9	-27.1 ± 0.9
ImmunoNPs	82.11 ± 1.79	179.8 ± 4.1	-24.3 ± 1.2

Phagocytic uptake of PCL NPs were compared with pegylated NPs containing varied quantity of PCL-PEG (5, 10, 15 and 20%) in terms of mean fluorescence intensity after 60, 120 and 240 min as shown in figure 5.5 (a), (b) and (c), respectively. Pegylated NPs displayed resistance to phagocytic uptake than non-pegylated NPs. After 1 h, uptake of PCL NPs was 1.33, 2.30 and 9.06 times more than PCL-PEG (5%), PCL-PEG (15%) and PCL-PEG (20%) NPs (figure 5.6). Phagocytic uptake of NPs were performed at three different time points to determine phagocytosis kinetics and it was found that phagocytosis increased in a time dependent manner. Small increase in uptake was observed with increase in time, but overall uptake decreased with increase in PEG content as reported by Tseng et al. [Chaudhari et al. 2012c; Mosqueira et al. 1999]. As discussed previously, the phagocytic uptake study with both the pegylated polymers (PLGA and PCL) showed lesser uptake with increased concentration of PEG.

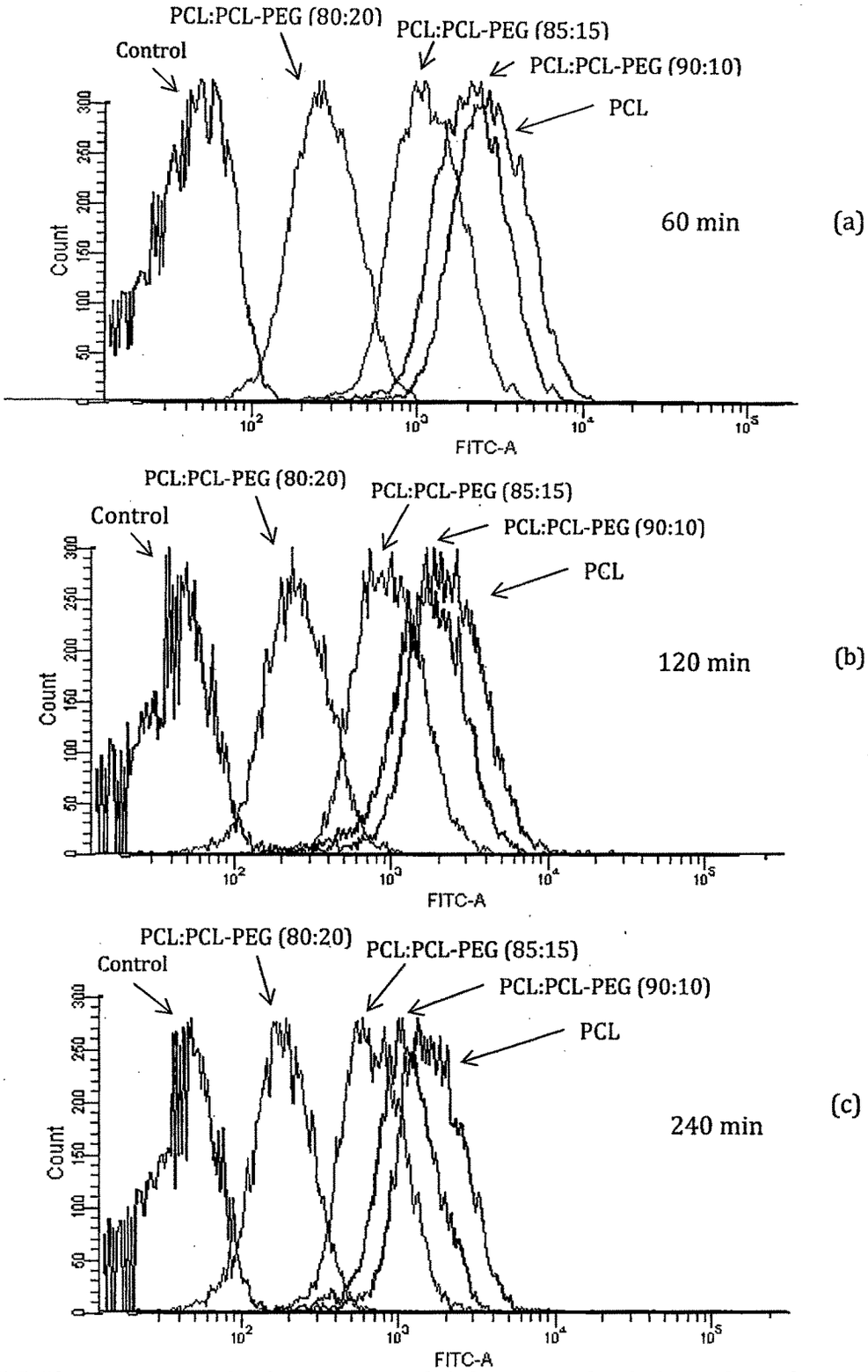

Figure 5.5 Phagocytic uptake histograms of 6-Coumarin loaded NP formulations by human acute monocytic leukemia cell line (THP1) after incubation for (a) 60, (b) 120 and (c) 240 min using FACS.

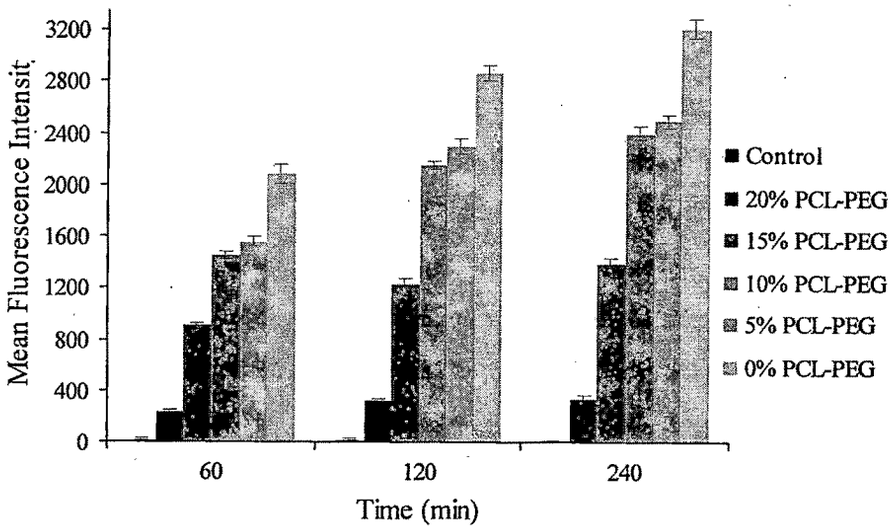

Figure 5.6 Phagocytic uptake of 6-coumarin loaded PCL and pegylated PCL NPs using Human acute monocytic leukemia cell line, THP-1 after incubation for 60, 120 and 240 min using FACS. Data presented as Mean ± SD, n=3.

The in vitro drug release studies from different nanoparticulate formulations were performed in PBS pH 7.4. Pegylated PCL NPs showed faster release as compared with non-pegylated NPs. In vitro release of EXE from drug suspension and NPs is shown in figure 5.7. Within 3 h, 71.36 ± 1.23% drug release occurred from plain drug suspension, whereas only 20.06 ± 1.31% and 24.88 ± 1.13% drug released from PCL and pegylated PCL NPs, reaching 44.89 ± 1.3% and 52.22 ± 3.1% after 120 h and 70.67 ± 1.76% and 83.26 ± 0.85% after 240 h, respectively indicative of sustained release. The drug release from NPs followed biphasic release model with an initial burst release for about 3 h followed by sustained release for more than 240 h. Pegylated PCL NPs showed faster release when compared to PCL NPs due to the presence of hydrophilic PEG chains around the NPs, causing increased diffusion of water to the core of particles. The regression coefficient of the plot of log M_t/M_∞ versus log t for PCL and pegylated PCL NPs was found to be 0.942 and 0.952 with value of release exponent (n) as 0.303 and 0.306, respectively. The n value is the release exponent which characterizes the transport mechanism and if its value is less than 0.5, it indicates Fickian release. Hence, it can be concluded that the release of ATZ from NPs was by Fickian diffusion.

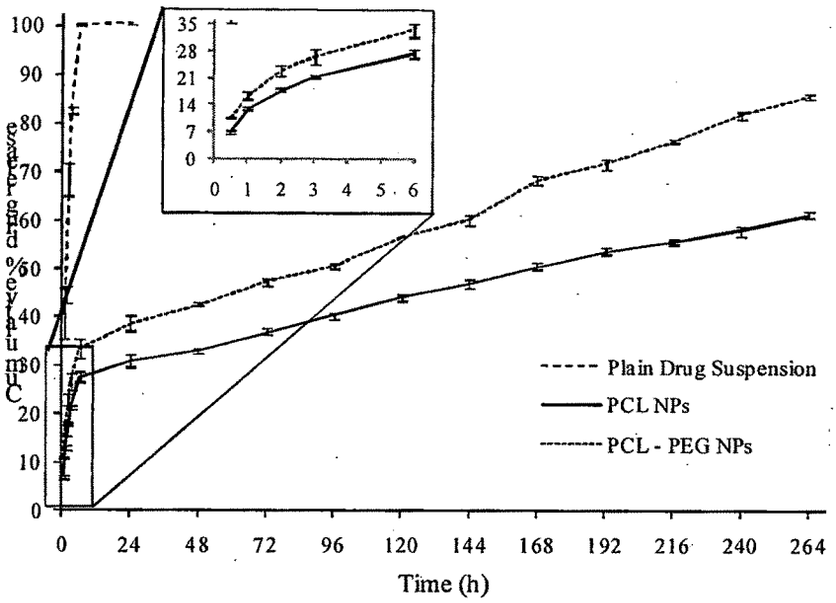

Figure 5.7 Drug release profile of EXE from plain drug suspension, PCL NPs and pegylated PCL NPs across semi-permeable membrane using the dialysis bag diffusion technique in phosphate buffered saline (pH 7.4). The values represent mean ± S.D. of three batches.

5.4.6 Physicochemical characterization of ImmunoNPs

EXE loaded pegylated PCL NPs were conjugated with anti-estrogen receptor monoclonal antibody for targeting breast tumor. For conjugation of Ab to pegylated PCL NPs, two-step EDC-NHS activation method was used. In this method, amino groups of monoclonal antibody were conjugated to carboxyl groups of PEG through an amide bond formation [Kocbek P 2007]. It was estimated that approximately 67 Ab molecules were present on each NP [Olivier et al. 2002].

EXE was successfully loaded in pegylated PCL NPs prior to Ab conjugation and no significant loss in drug content was observed after surface functionalization with Ab. However, slight increase in PS was observed. The PS increased from 168.9 ± 2.9 to 179.8 ± 4.1 nm with slight decrease in zeta potential from -27.1 ± 0.9 to -24.3 ± 1.2 mV. Poly dispersity index before and after Ab conjugation was less than 0.1 indicating unimodal distribution of particles. A similar trend was observed by Das et al. and Tseng et al. when they conjugated antibody on PLGA and gelatin NPs, respectively [Das and Sahoo 2011; Tseng et al. 2007]. TEM image showed discrete spherical particles with monodisperse size of about 100 nm (figure 5.8). The higher hydrodynamic diameter of

NPs achieved by dynamic light scattering (Zetasizer NanoZS) analysis as compared to the size obtained by TEM analysis is possibly contributed by the hydration of the surface associated PEG.

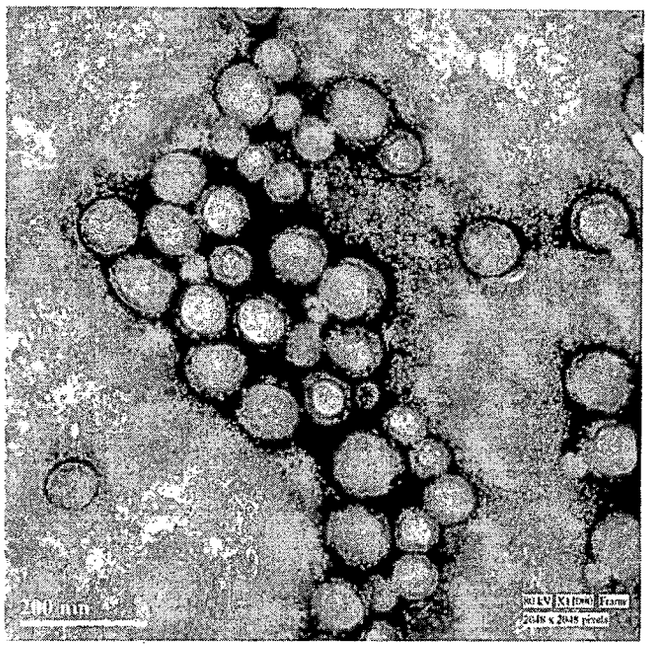

Figure 5.8 TEM image of EXE loaded pegylated PCL ImmunoNPs.

5.5 References

Acharya S, Dilnawaz F, Sahoo SK. 2009. Targeted epidermal growth factor receptor nanoparticle bioconjugates for breast cancer therapy. Biomaterials 30(29):5737-5750.

Avgoustakis K, Beletsi A, Panagi Z, Klepetsanis P, Livaniou E, Evangelatos G, Ithakissios DS. 2003. Effect of copolymer composition on the physicochemical characteristics, in vitro stability, and biodistribution of PLGA–mPEG nanoparticles. Int. J. Pharm. 259(1–2):115-127.

Chaudhari KR, Kumar A, Khandelwal VKM, Mishra AK, Monkkonen J, Murthy RSR. 2012. Targeting efficiency and biodistribution of zoledronate conjugated docetaxel loaded pegylated PBCA nanoparticles for bone metastasis. Advanced Functional Materials 22(19):4101-4114.

Chaudhari KR, Kumar A, Megraj Khandelwal VK, Ukawala M, Manjappa AS, Mishra AK, Monkkonen J, Ramachandra Murthy RS. 2012. Bone metastasis targeting: A novel

approach to reach bone using Zoledronate anchored PLGA nanoparticle as carrier system loaded with Docetaxel. J. Controlled Rel. 158(3):470-478.

Chaudhari KR, Ukawala M, Manjappa AS, Kumar A, Mundada PK, Mishra AK, Mathur R, Monkkonen J, Murthy RS. 2012c. Opsonization, biodistribution, cellular uptake and apoptosis study of PEGylated PBCA nanoparticle as potential drug delivery carrier. Pharm. Res. 29(1):53-68.

Das M, Sahoo SK. 2011. Epithelial cell adhesion molecule targeted nutlin-3a loaded immunonanoparticles for cancer therapy. Acta. Biomater. 7(1):355-369.

Josephson L, Tung CH, Moore A, Weissleder R. 1999. High-efficiency intracellular magnetic labeling with novel superparamagnetic-Tat peptide conjugates. Bioconjug. Chem. 10(2):186-191.

Kanchan V, Panda AK. 2007. Interactions of antigen-loaded polylactide particles with macrophages and their correlation with the immune response. Biomaterials 28(35):5344-5357.

Kocbek P, Obermajer N, Cegnar M, Kos J, Kristl J. 2007. Targeting cancer cells using PLGA nanoparticles surface modified with monoclonal antibody. J. Controlled Rel. 120(1-2):18-26.

Mosqueira VC, Legrand P, Gref R, Heurtault B, Appel M, Barratt G. 1999. Interactions between a macrophage cell line (J774A1) and surface-modified poly (D,L-lactide) nanocapsules bearing poly(ethylene glycol). J. Drug Target. 7(1):65-78.

Muhlfeld C, Rothen-Rutishauser B, Vanhecke D, Blank F, Gehr P, Ochs M. 2007. Visualization and quantitative analysis of nanoparticles in the respiratory tract by transmission electron microscopy. Part. Fibre Toxicol. 4:11.

Olivier JC, Huertas R, Lee HJ, Calon F, Pardridge WM. 2002. Synthesis of pegylated immunonanoparticles. Pharm. Res. 19(8):1137-1143.

Tseng CL, Wang TW, Dong GC, Yueh-Hsiu Wu S, Young TH, Shieh MJ, Lou PJ, Lin FH. 2007. Development of gelatin nanoparticles with biotinylated EGF conjugation for lung cancer targeting. Biomaterials 28(27):3996-4005.